Robotica (2012) volume 30, pp. 1041–1048. © Cambridge University Press 2011
doi:10.1017/S0263574711000774

Optimal design of 6-DOF eclipse mechanism based on task-oriented workspace

Donghun Lee†, Jongwon Kim‡ and TaeWon Seo§*

†*Mechatronics Center, Samsung Heavy Industry, Daejeon, Republic of Korea*
‡*School of Mechanical and Aerospace Engineering, Seoul National University, Seoul, Republic of Korea*
§*School of Mechanical Engineering, Yeungnam University, Gyeongsan, Republic of Korea*

(Accepted June 15, 2011. First published online: July 25, 2011)

SUMMARY

We present a new numerical optimal design for a redundant parallel manipulator, the eclipse, which has a geometrically symmetric workspace shape. We simultaneously consider the structural mass and design efficiency as objective functions to maximize the mass reduction and minimize the loss of design efficiency. The task-oriented workspace (TOW) and its partial workspace (PW) are considered in efficiently obtaining an optimal design by excluding useless orientations of the end-effector and by including just one cross-sectional area of the TOW. The proposed numerical procedure is composed of coarse and fine search steps. In the coarse search step, we find the feasible parameter regions (FPR) in which the set of parameters only satisfy the marginal constraints. In the fine search step, we consider the multiobjective function in the FPR to find the optimal set of parameters. In this step, fine search will be kept until it reaches the optimal set of parameters that minimize the proposed objective functions by continuously updating the PW in every iteration. By applying the proposed approach to an eclipse-rapid prototyping machine, the structural mass of the machine can be reduced by 8.79% while the design efficiency is increased by 6.2%. This can be physically interpreted as a mass reduction of 49 kg (the initial structural mass was 554.7 kg) and a loss of 496 mm^3/mm in the workspace volume per unit length. The proposed optimal design procedure could be applied to other serial or parallel mechanism platforms that have geometrically symmetric workspace shapes.

KEYWORDS: Optimal design; Task-oriented workspace; Partial workspace; Eclipse mechanism; Parallel kinematic mechanism; Conjugate gradient method; Fine and coarse search; Structural mass.

1. Introduction

Before considering optimal design, it is necessary to define the workspace to be used in the optimal design. Kumar and Waldron proposed optimal design and analysis on reachable and dexterous workspaces.[1–6] A reachable workspace is a position set of end-effectors in which an end-effector can reach without considering orientation, and a dexterous workspace is a position set of end-effectors in which an end-effector can reach with a full rotational capability of 360°. Haug *et al.* proposed a composite workspace that requires a specified working capability in joint space for all sets of points,[7,8] and a Jacobian approach that determines the workspace boundary in terms of rank deficiency. Pond and Carretero also proposed a Jacobian approach that determines the workspace in terms of the condition number of the Jacobian matrix.[9] Bonev and Ryu proposed the orientation workspace—the set of all attainable orientations of an end-effector about a fixed point.[10] We note that the previous concepts of the workspace are not suitable in our proposed optimal design approach since a direct consideration on the prescribed rotational capability of the end-effector represents good performance in determining the workspace boundary required in the tasks.

In this study, the task-oriented workspace (TOW) and its partial workspace (PW) are crucial in efficiently obtaining the optimal design. Since we need only 90° of rotational capability to achieve five-face machining of the eclipse-rapid prototyping (RP) machine, the TOW can be obtained by excluding useless orientations of the end-effector. Here, the TOW can be defined as a position set of the end-effector such that the end-effector can reach with a predefined rotational capability. In the eclipse mechanism, a 90° rotational capability is predefined. Obviously, the TOW is worth to use in determining useful workspace for the five-face machining for the eclipse-RP machine.

Even if we only considered prescribed orientations in the end-effector space, workspace searching is still a time-consuming procedure. Thus, in order to reduce the computational cost, the PW, which can be considered as a cross-sectional area of the TOW, is proposed to calculate the distance between the TOW and the workpiece without exhaustively searching the possible position candidates in full range of the TOW. Few studies on the proposed geometric treatments for the manipulator workspace were found in the literature; however, this topic seems to be a worthwhile subject to investigate and should be a great help in the optimal design.

Using the proposed geometric treatments on the manipulator workspace, we simultaneously considered structural mass and design efficiency as objective functions with respect to maximizing the mass reduction and minimizing the loss of design efficiency. The design involves two steps: coarse and fine searches. In the coarse search

* Corresponding author. E-mail: taewon_seo1@yu.ac.kr

https://doi.org/10.1017/S0263574711000774 Published online by Cambridge University Press

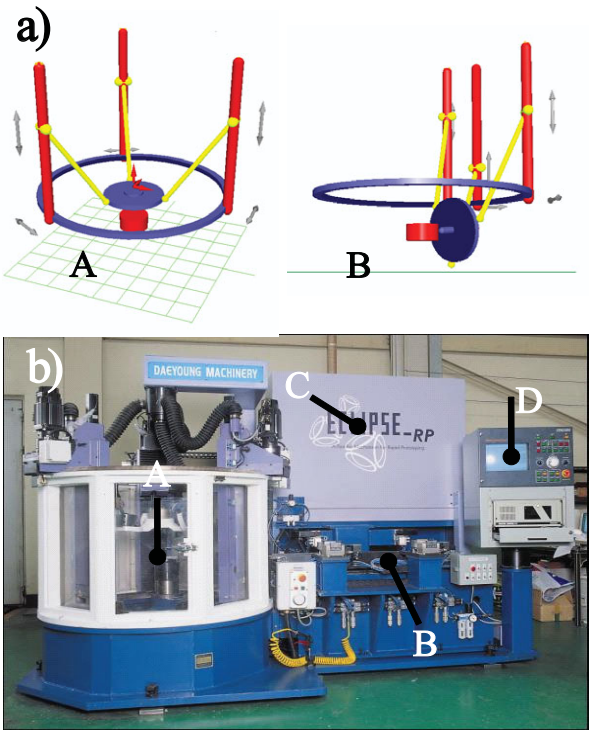


Fig. 1. (Colour online) Eclipse mechanism and machine. (a) Posture of 0° tilting, A and 90° tilting, B. (b) Eclipse-RP machine. A: Eclipse mechanism-based machine tool, B: Material feeder, C: Controller and drivers, D: User interface based on PC.

step, we find feasible parameter regions (FPRs) where the predefined constraints are satisfied. In the find search step, we analyze the objective function in the FPRs to obtain the final optimal parameter set. The proposed two-step procedure simplifies the optimal design problem by separating the complicated constraints and the objective function.

2. Kinematic Configuration

Parallel kinematic machines (PKMs) are widely researched due to their advantages and simplicity in solving inverse kinematics with high accuracy and high resolution.[11–13] However, some drawbacks exist, such as low stiffness, a small workspace, and limited rotational capability. An eclipse mechanism,[14] shown in Fig. 1(a), has been proposed to overcome the limited rotational capability of existing parallel mechanisms. The eclipse mechanism achieves 90° of rotational capability.

The inventors of the eclipse mechanism built the so-called eclipse-RP machine, which is a RP machine based on the eclipse mechanism, as shown in Fig. 1(b).[15] The machine performs excellent machining processes using its superior rotational capability. However, due to its design complexity, the machine is too big compared to the small workspace of the machine. Furthermore, mass due to unnecessary link lengths may result in more power consumption and low dynamic performance during the machining process. Therefore, an optimal design of the link lengths is required to reduce the mass and improve the design efficiency while satisfying the required workspace.

In this section, we introduce the kinematic configuration of the eclipse mechanism and define the kinematic design

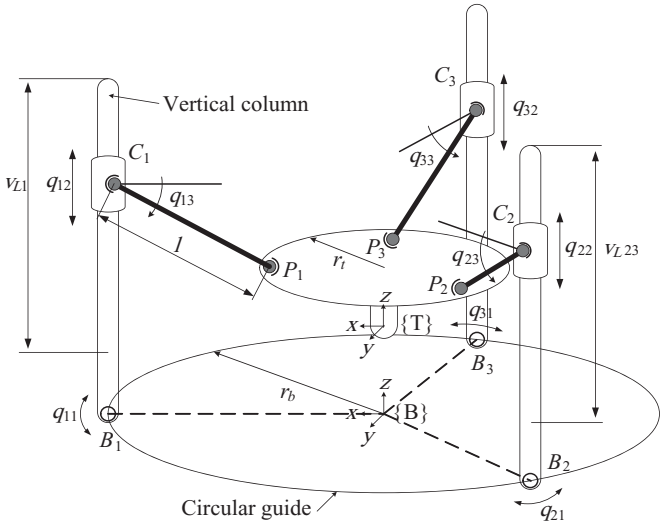


Fig. 2. Kinematic configuration of the eclipse mechanism.

parameters (DPs) to be optimized. Figure 2 shows the kinematic configuration of the eclipse mechanism. On the circular guide at the base, the mechanism consists of three chains connecting by a series of two-prismatic, rotational, and spherical (PPRS) joints. The last spherical joints are connected to the end-effector as shown in Fig. 2. The eclipse mechanism is overactuated to avoid singularities; thus, it has eight actuators, $q_{i_1}, q_{i_2} (i = 1, 2, 3)$ and $q_{j_3} (i = 1, 2)$, to achieve six degree of freedom (DOF) motion.[14]

{B} and {T} denote the base and tool frame, respectively. $B_i, C_i, P_i (i = 1, 2, 3)$ denote the position vectors of the vertical column on the circular guide, prismatic joint on the vertical column, and ball joint in the end-effector, respectively. $q_{i_1}, q_{i_2}, q_{i_3} (i = 1, 2, 3)$ denote the scalar joint values of the prismatic joint on the circular guide, the prismatic joint on the vertical column, and the rotational joint of the links, respectively. v_{L_1} and $v_{L_{23}}$ represent lengths of the vertical columns, and r_b and r_t represent the radii of the circular guide and the end-effector, respectively. The kinematic DPs are summarized in Table I.

The kinematic equations that are functions between the active joints $(q_{i_1}, q_{i_2} (i = 1, 2, 3))$ and pose of the end-effector (p_t: position vector of the end-effector, R_t: rotation matrix of the end-effector). The kinematics equations are derived in detail in ref. [14]. We used the equations as follows:

$$(p_t, R_t) = FK(q_{i1}, q_{i2}) \text{ and } (q_{i1}, q_{i2}) = IK(p_t, R_t), \quad i = 1, 2, 3. \tag{1}$$

Here, the *FK* and *IK* are from forward kinematics and inverse kinematics, respectively. The *FK* can be solved by numerical iterations and the *IK* are solved by an analytical method. The *IK* are used by our algorithm to calculate the workspace as described in Section 4. The DPs of the eclipse-RP machine are summarized in Table I. We introduce $q_i (i =$ 1to5), which are values to be used in the optimal design procedure. It is important to note that the DPs in Table I were also selected to satisfy the required workspace; however, the DPs were not efficiently selected since they were determined

https://doi.org/10.1017/S0263574711000774 Published online by Cambridge University Press

Table I. Kinematic variables of eclipse-RP machine.

Design parameters	Parameters in Fig. 2	Values (mm)	Physical meaning
q_1	l_i	250	The connecting links, $i = 1, 2, 3$.
q_2	v_{L_1}	702	The first vertical column.
q_3	$v_{L_{23}}$	335	The second and third vertical columns.
q_4	r_b	360	The radius of the circular guide.
q_5	r_t	245	The radius of the tool plate.

by a trial-and-error procedure. The q_i values are the values to be optimized.

3. Optimal Design Problem Definition

3.1. Multiobjective function

The objective of the study is to decrease the structural mass of the eclipse mechanism and to increase the design efficiency (i.e., the workspace volume per unit length of the kinematic DPs) simultaneously. The objective function is composed of two components. The first component is defined as follows:

$$f_1(q) = \frac{Q_L}{Q_{L,0}}, \tag{2}$$

$$Q_L = \frac{\sum_{i=1}^{n} q_i}{\sqrt[3]{V_{\mathrm{TOW}}}}, \tag{3}$$

where V_{Tow} denotes the volume of the TOW, subscript "0" denotes the initial design state, and $f_1(q)$ represents the rate of change in mechanical design efficiency[16–18] for the new design with respect to the initial design. However, in spite of the importance of weight change, its effect in changing the design parameters cannot be fully considered in $f_1(q)$. Thus, $f_2(q)$, which represents the rate of mass reduction, was applied to simultaneously minimize the structural weight. Thus,

$$f_2(q) = \frac{\sum_{i=1}^{n} \rho_i A_i q_i}{\sum_{i=1}^{n} \rho_i A_i q_{0,i}}, \tag{4}$$

where ρ_i denotes the densities of the materials, A_i denotes the area of each link, and the subscript "0" in q_i denotes the initial design parameter value. By introducing $f_1(q)$, we can expect to reduce the structural mass effectively. The proposed objective functions were nondimensionalized by dividing them by the values of initial design state. Consequently, the objective function is defined as follows:

$$\text{Minimize}: F(q) = \omega_1 \cdot \frac{\sum_{i=1}^{n} q_i \cdot \sqrt[3]{V_{\mathrm{TOW},0}}}{\sum_{i=1}^{n} q_{i,0} \cdot \sqrt[3]{V_{\mathrm{TOW}}}} + \omega_2 \cdot \frac{\sum_{i=1}^{n} \rho_i A_i q_i}{\sum_{i=1}^{n} \rho_i A_i q_{0,i}}, \tag{5}$$

where w_1 and w_2 are nonnegative weights on each component. We chose equal weights of 0.5 for each weight.

3.2. Constraints

There are six constraints to be defined. Each constraint was used to find FPRs, as described in Section 5:

(A) *Stroke of the prismatic joints*: The prismatic joints on the vertical columns should satisfy the following constraints t satisfy the joint limit:

$$q_{i2}^{\mathrm{lower}} \le -D_i + \sqrt{D_i^2 - E_i} \le q_{i2}^{\mathrm{upper}},$$
$$\text{where } D_i = (B_i - P_i)^{\mathrm{T}} \cdot n_z \text{ and } E_i = \|B_i - P_i\|^2 - l^2, \tag{6}$$

where the n_z denotes normal vector in z-direction. q_{i2}^{lower} and q_{i2}^{upper} are mechanical limit of each column.

(B) *Preventing interference between vertical columns*: To avoid interference between vertical columns, we defined a constraint as follows:

$$\|q_{11} - q_{21}\|, \ \|q_{21} - q_{31}\|, \text{ and } \|q_{31} - q_{11}\| \ge 30^\circ. \tag{7}$$

(C) *Ball joint limit*: The mechanical limitation of the ball joint is –55°. To satisfy the mechanical limit, we derived a constraint equation using the following procedure. First, the geometric centerline for each ball joint in base frame {B} can be calculated as follows:

$$\begin{cases} \zeta_1 = \mathbf{R}_t \times [\cos\cos(\vartheta_1), 0, \sin\sin(\vartheta_1)]^{\mathrm{T}}, \\ \zeta_2 = \mathbf{R}_t \times \mathbf{R}_{z,120} \times [\cos\cos(\vartheta_2), 0, \sin\sin(\vartheta_2)]^{\mathrm{T}}, \\ \zeta_3 = \mathbf{R}_t \times \mathbf{R}_{z,-120} \times [\cos\cos(\vartheta_3), 0, \sin\sin(\vartheta_3)]^{\mathrm{T}}, \end{cases} \tag{8}$$

where ϑ_i represents the angle of the centerline of ball joint i in the tool frame {T}; i.e., $\vartheta_1 = 94.5^\circ$, and ϑ_2 and $\vartheta_2 = 20^\circ$. The $\mathbf{R}_{z,120}$ and $\mathbf{R}_{z,-120}$ denote 120 or -120° rotated vectors of third column of $\mathbf{R}_t$. Finally, the mechanical limitation constraint is defined as follows:

$$q_{ib} = \arccos\left(\frac{(\mathbf{P}_{\mathrm{i}} - \mathbf{C}_{\mathrm{i}}) \cdot \zeta_i}{(\mathbf{P}_{\mathrm{i}} - \mathbf{C}_{\mathrm{i}}) \cdot \zeta_i}\right) \le \pm 55^\circ, i = 1, 2, 3. \tag{9}$$

(D) *Preventing interference between the spindle holder and the pallet*: Mechanical interference between the spindle holder and the pallet should be avoided for machining processes. The constraint can be defined as follows:

$$\text{where} \quad \begin{array}{l} d_{\mathrm{holder}} = \sqrt{\mathbf{p}_{\mathrm{holder}}(1)^2 + \mathbf{p}_{\mathrm{holder}}(2)^2} \ge r_{\mathrm{pallet}}, \\ \mathbf{p}_{\mathrm{holder}} = \mathbf{R}_{\mathrm{t}}[r_{\mathrm{b}}, 0, l_{\mathrm{tool}} - h_{\mathrm{holder}}]^{\mathrm{T}} + \mathbf{p}_{\mathrm{t}}, \end{array} \tag{10}$$

where l_{tool}, h_{holder}, and r_{pallet} denote the length of the tool (170 mm in the eclipse-RP), the height of holder (85 mm in the eclipse-RP), and the allowable radius of the pallet, respectively. The resulting d_{holder}, which physically represents the distance from the center of the pallet to the tool, should be larger than the radius of the pallet.

(E) 90° *rotational capability*: The rotational capability of the eclipse machine is the main characteristic of the machine, and it should be satisfied. Figure 3 describes the rotational capability. Rotation about the spindle axis is not required in the machine process. The required capability can be defined

https://doi.org/10.1017/S0263574711000774 Published online by Cambridge University Press

Table II. Design constraints in terms of workspace margins.

Parameters	Constraints	Design status
Ω_r	$0_{\text{mm}} \leq \Omega_r \leq 2\,\text{mm}$	Unsatisfied (12.4 mm)
Ω_{zl}	$0_{\text{mm}} \leq \Omega_{zl} \leq 5\,\text{mm}$	Unsatisfied (30 mm)
Ω_{zu}	$0_{\text{mm}} \leq \Omega_{zu} \leq 5\,\text{mm}$	Satisfied (5 mm)

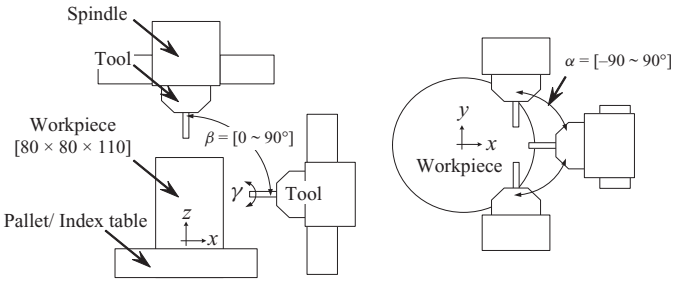


Fig. 3. The required rotational capability in base frame {B}. (a) View in *XZ*-plane; (b) view in *XY*-plane.

as follows:

$$\begin{cases} -90^\circ \leq \alpha \leq 90^\circ, \\ 0^\circ \leq \beta \leq 90^\circ : \text{tilting angle}, \\ \gamma : \text{rolling angle}, \end{cases} \tag{11}$$

where α, β, and γ are the *Z–Y–Z* Euler angles.

(F) *Workspace margins*: The constraint regarding the gap distance between the workpiece and the TOW in all directions should be considered to be the most important issue in this study. The margins are established with respect to tolerances in the manufacturing of eclipse parts and uncertainties during machining processes by the eclipse machine, as shown in Table II. Since the workspace of the eclipse mechanism is a cylindrical shape, there are three margins in the radius direction (Ω_r), and lower and upper margins in the longitudinal direction (Ω_{zl},Ω_{zu}). Note that the eclipse-RP machine does not satisfy the required workspace margin.

4. Workspace Analysis

The computation cost in calculating workspace of a manipulator is important factor in workspace analysis. Generally, an exhaustive search method is used, but this is definitely inefficient in terms of computational cost since it should check all possible point candidates inside the possible work.

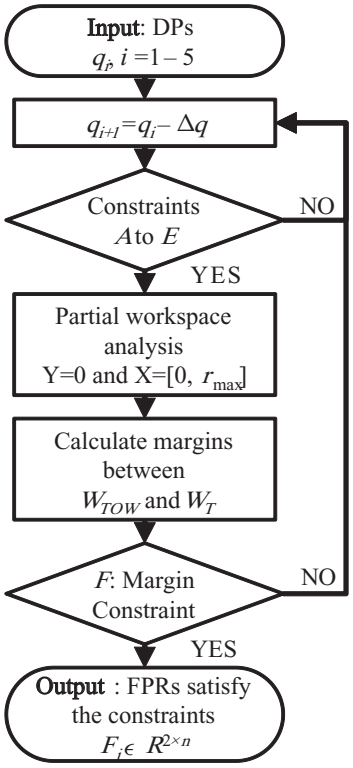


Fig. 5. Exhaustive coarse search to find FPRs.

To approach this work from a different angle, we propose the TOW, PW, and maximally inscribed parallelepiped (MIP) to the proposed workspace. The PW is a subspace of the TOW. The TOW and its PW are important for efficiently obtaining the optimal design. Since we only need the prescribed rotational capability (shown in Fig. 3) to achieve five-face machining using the eclipse-RP, the TOW can be obtained by excluding useless orientations of the end-effector. Thus, the TOW just considers the end-effector orientations described in a constraint section—90° rotational capability—for all points in a scattered point cloud near the robot base.

Even if we consider only prescribed orientations in the end-effector space, workspace searching is still a time-consuming procedure since all scattered points should be checked. Thus, to reduce computational cost, we propose the PW, which can be considered as a cross-sectional area of the TOW as shown in Fig. 4, and the MIP, to calculate the distance between the TOW and the workpiece. In this scheme, it is not necessary

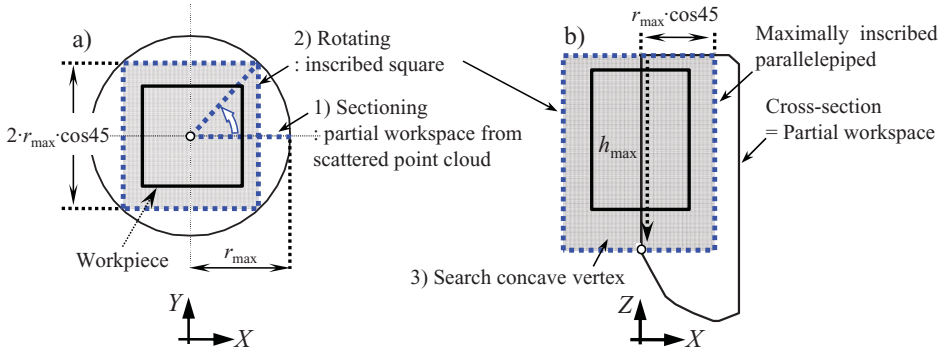


Fig. 4. (Colour online) Concept of the PW and calculation of the MIP. (a) Section view in *XZ*-plane; (b) Section view in *XY*-plane (the TOW is calculated by rotating the PW).

https://doi.org/10.1017/S0263574711000774 Published online by Cambridge University Press

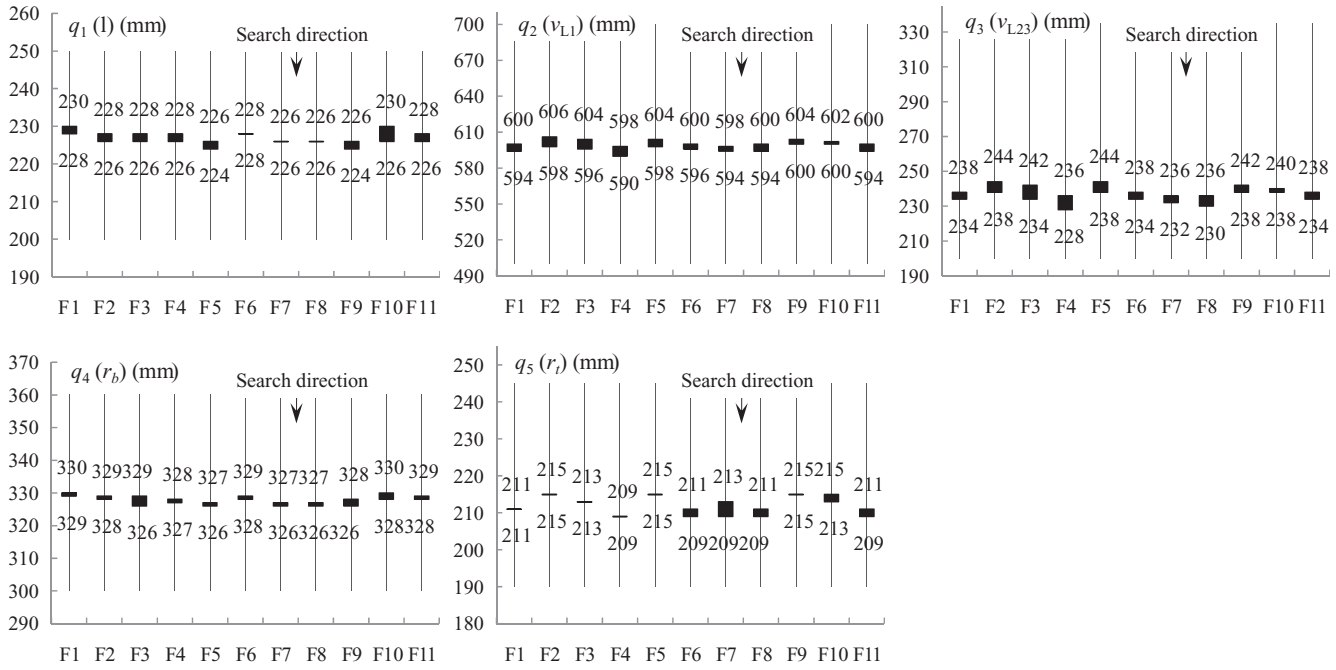


Fig. 6. Coarse search and corresponding results of FPRs.

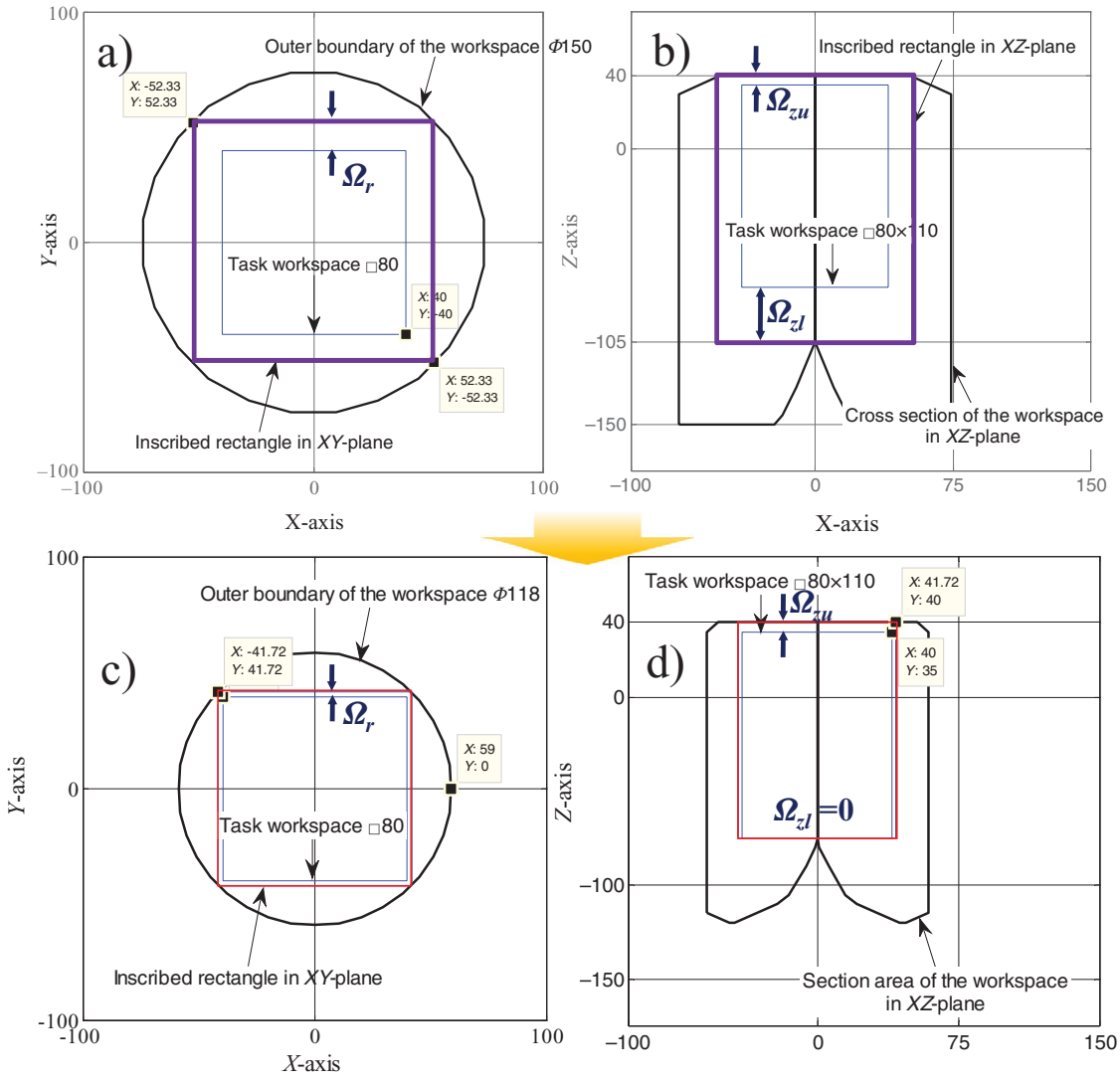


Fig. 7. (Colour online) Result of the coarse search: (a), (b) from initial design, and (c), (d) from FPRs. Margins are calculated as follows: $\Omega_r = 1.72$ mm, $\Omega_{zu} = 5$ mm, and $\Omega_{zl} = 0$ mm.

https://doi.org/10.1017/S0263574711000774 Published online by Cambridge University Press

to search the full range of the TOW from the scattered point cloud for every iteration.

As previously mentioned, the constraint regarding workspace margin is the most important subject in this study. To efficiently calculate it, the MIP of the PW is proposed. As shown in Fig. 4, we obtained the PW from section of the TOW for the *XZ*-plane, and then, by rotating the PW, the gap distance can be calculated from $r_{\max} \cdot \cos \pi / 4 - l_{\text{workpiece}}$, where $l_{\text{workpiece}}$ denotes the length of one side of the inscribed parallelepiped. Finally, the concave vertex, which seems to be the maximum height of the inscribed parallelepiped, can be found by stretching the search in *Z*-direction.

We note that the proposed PW and search path planning for finding the MIP will be a great help in reducing the computational efforts, since much effort was direct toward quickly finding a feasible design parameter space that satisfies all of the given design constraints from the initial design. Few studies on the proposed geometric treatments for a manipulator workspace were found in the literature.

5. Optimal Design Procedure

5.1. Coarse search: Finding the FPRs

In the coarse search stage, we find the FPRs that satisfy the prescribed design constraints without consideration of the objective functions. This procedure is shown in Fig. 5. As previously mentioned, to reduce computational time, the PW and MIP of the TOW are introduced in this stage. The coarse search produced 11 FRPs for five design parameters.

Figure 6 represents the corresponding results of FPRs obtained from the coarse search stage and the search direction from the initial design parameters, respectively. The FPRs still remained independent from the objective function described by Eq. (5). However, by formulating the penalty function[19–20] from the obtained FPRs and embedding it into original objective functions, the constrained optimization problem described by Eq. (5) was transformed into an unconstrained problem as shown in Eq. (12)

$$\begin{aligned} \text{Minimize}: F(q) &= \omega_1 \cdot \frac{\sum_{i=1}^{n} q_i \cdot \sqrt[3]{V_{\text{TOW},0}}}{\sum_{i=1}^{n} q_{i,0} \cdot \sqrt[3]{V_{\text{TOW}}}} \\ &+ \omega_2 \cdot \frac{\sum_{i=1}^{n} \rho_i A_i q_i}{\sum_{i=1}^{n} \rho_i A_i q_{0,i}} + R\{\max(0, g_j(q_i)) + |h_k|\} \\ \textit{where}, & \begin{cases} g_1(q_i) = q_i^{\text{lower}}|_{j=1}^{m} - q_i \le 0 \\ g_2(q_i) = q_i - q_i^{\text{upper}}|_{j=1}^{m} \le 0 \\ h_k = q_i - \text{constant}. \end{cases} \end{aligned} \tag{12}$$

To examine the effect of coarse search under FPRs, a workspace analysis was conducted and is represented in Fig. 7. The figure shows that the gap distances in all directions are within the ranges of the constraints, and the FPRs can be quickly obtained using the PW and inscribed parallelepiped without full searching of the TOW at every iteration.

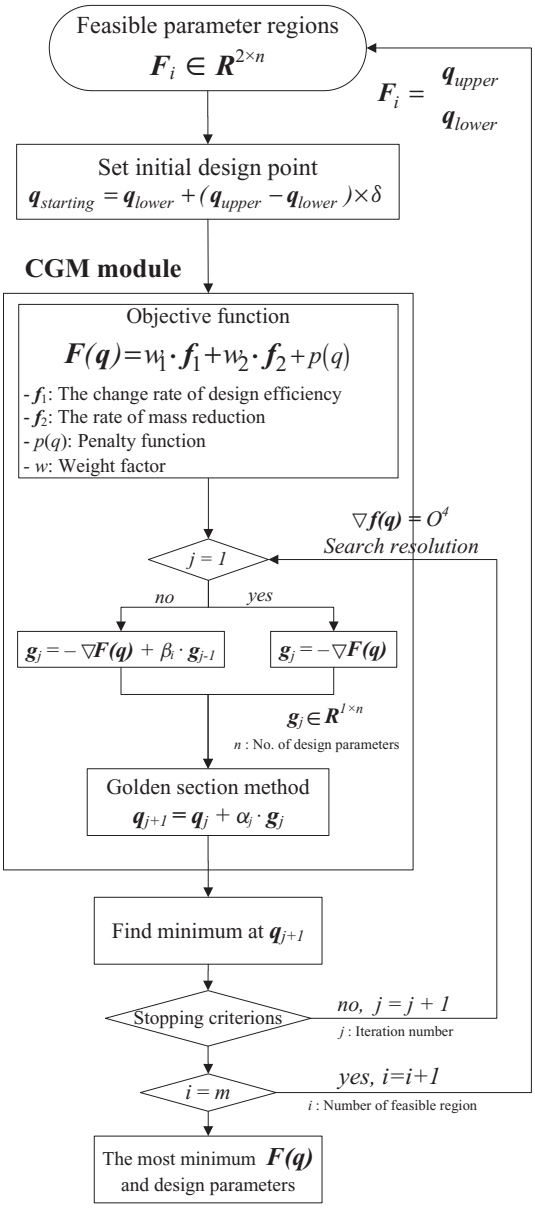


Fig. 8. Optimal design step II: fine search using a gradient-based method.

5.2. Fine search: Analyzing the objective function

We analyzed the objective function of Eq. (5) considering the structural mass and the design efficiency in the calculated FPRs. We adopted the conjugate gradient method (CGM) to find the optimal DPs. The procedure of fine search based on CGM is shown in Fig. 8. In the FPRs, the DPs go into the CGM module as shown in Fig. 8, and the iterations is continued until the stopping criteria is satisfied. Here, the stopping criteria are very important in obtaining reasonable solutions.

The stopping criteria in the CGM module are defined as follows: (1) $||F(q_{i+1}) - F(q_i)||$, which represents the variation of the objective function between i and $i + 1$, is set to 1.0^{-5} in light of the order of 10^{-1} mm for $F(q)$; (2) $\Delta q^{\mathrm{T}} \Delta q$, which represents the variation of the design parameters, is set to 1.0^{-2} mm; and (3) $\nabla F(q_{i+1})^{\mathrm{T}} \nabla F(q_{i+1})$, which represents the search length in the iterations, is set to 1.0^{-5} since the total search length should be decided by multiplying α_{i} and $\nabla F(q_{i+1})$.

https://doi.org/10.1017/S0263574711000774 Published online by Cambridge University Press

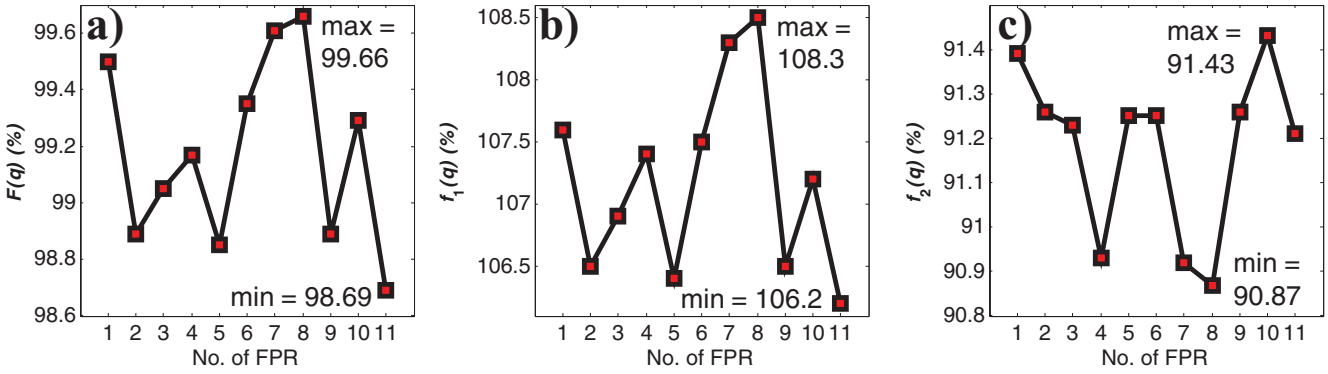


Fig. 9. (Colour online) Profile of the objective functions over all FPRs.

As a result of the procedure shown in Fig. 8, the optimization results for all the FPRs are shown in Fig. 7. The optimal design result shows that the loss of design efficiency increases as the design parameters decrease, whereas the mass reduction increases. Also, the maximum deviation of the mass reduction over the FPRs is just 0.59% compared to 2.3% in the loss of design efficiency, as shown in Fig. 9. Here, we conclude that the result of optimal design from the fine search is more dependent on the loss of design efficiency, since the results for mass reduction over the FPRs are in the vicinity of 0.59%. Consequently, as shown in Fig. 9, the optimal values of $F(q)$ are located in FPR # 11. Therefore, the DPs are the optimal of FPR # 11 that are the final solution of the optimization problem.

Table III. Optimized design parameters (in mm).

Design parameters	$q_1(l)$	$q_2(v_{L1})$	$q_3(v_{L23})$	$q_4(r_b)$	$q_5(r_t)$
Initial design	250	702	340	370	245
Optimal design	226.2	596.9	235.7	328.0	209.9
Reduced link lengths	−23.8	−105.2	−104.3	−42.0	−35.1

Table IV. Optimized margins in the r- and z-directions (in mm).

Margins	Ω_r	Ω_{zi}	Ω_{zu}
Initial design	12.3	30	5
Optimal design	1.7	0	5
Variations	10.6	30	0

6. Results

Finally, we obtained the optimal set of DPs in FPR # 11. Table III shows the final optimal set of DPs, and Fig. 10 shows the optimized TOW of the Eclipse mechanism. As expected, all the DPs decreased. Note that two DPs related to the vertical column (q_2 and q_3) significantly decreased in length. The other three DPs also decreased to reduce the structural mass and the design efficiency. Previously, in Fig. 7 in Section 5.1, the TOW of the eclipse-RP machine and the TOW calculated from the optimal DPs were presented. Note that even though

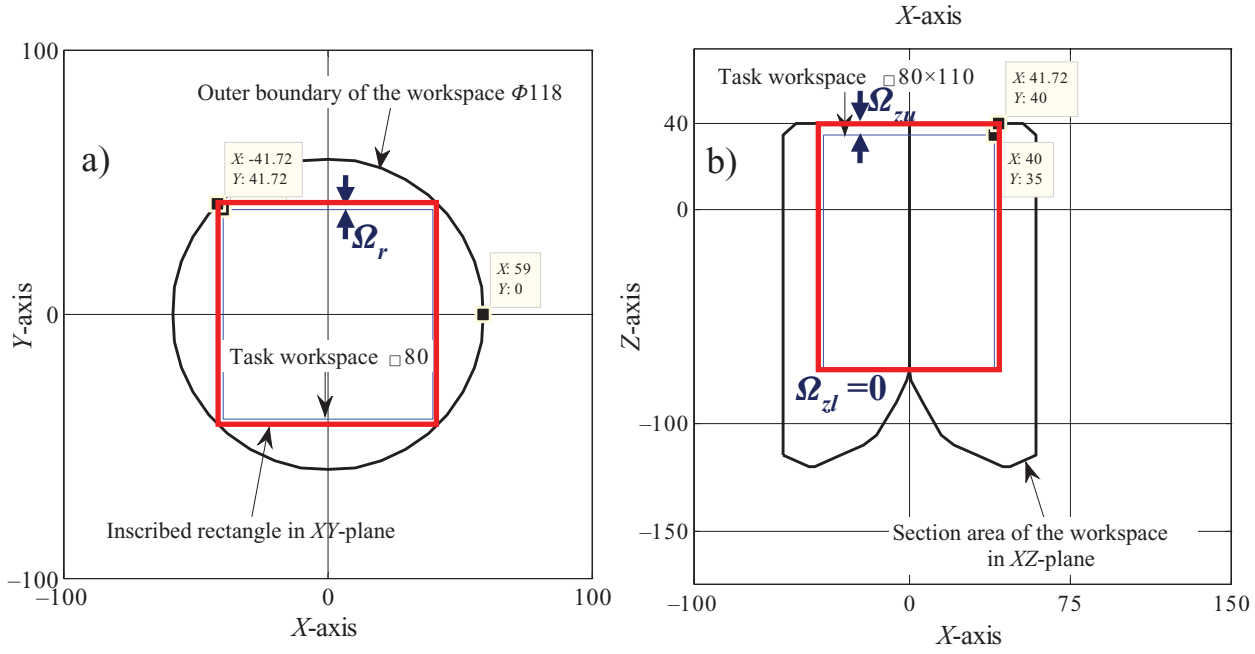


Fig. 10. (Colour online) Optimized task-oriented workspace of the Eclipse mechanism.

https://doi.org/10.1017/S0263574711000774 Published online by Cambridge University Press

Table V. Resulting objective functions.

	$f_1(q)$: Design efficiency		$f_2(q)$: Mass reduction	
	Objective function (%)	Physical variation (mm^3/mm)	Objective function (%)	Physical variation (kg)
Initial design	100	750	100	554.7
Optimal design	+6.17	1,245 (+495 mm^3/mm)	−8.79	505.4 (−49.3 kg)

the TOW was reduced, the required margins are satisfied as summarized in Table IV.

The analysis results on the objective function are shown in Table V. The results show that we can expect a 6.17% increase in the design efficiency (which is physically 495 mm^3/mm of the TOW volume increase per unit length of DP), and an 8.79% decrease in the structural mass (which is physically a 49.3 kg decrease). We know that two components of the objective function efficiently worked as the objective function while the other constraints were satisfied.

7. Conclusion

We presented the results of an optimal design for the eclipse mechanism. We simultaneously considered the structural mass and design efficiency as objective functions to maximize mass reduction while minimizing the loss of design efficiency. The TOW and its PW were regarded as crucial in efficiently obtaining the optimal design by excluding useless orientations of the end-effector and by including just one cross-sectional area of the TOW. The proposed PW and search path planning to find a MIP were a great help in reducing computational efforts. This is because many calculations were needed to quickly find a feasible design parameter space that satisfied all the given design constraints from the initial design in the coarse search stage. As a result, the structural mass was reduced by 8.79% (physically, 49.3 kg), and the design efficiency was increased by 6.2% (physically, 495 mm^3/m). The procedure for optimal design described in this paper can be applied to other serial or parallel mechanism machines. The calculation algorithm for the TOW can also be applied to calculate the TOW of other mechanisms for specific applications.

Acknowledgments

This research was supported by the Brain Korea 21 project and the National Research Foundation of Korea(NRF) grant funded by the Korea government(MEST) (No. 2010-0027809). The authors thanks Robust Design Engineering Laboratory members of Seoul National University for their supports on this study.

References

1. K. Y. Tsai, T. K. Lee and K. D. Huang, "Determining the workspace boundary of 6-DOF parallel manipulators," *Robotica* **24**, 605–611 (2006).
2. J. P. Merlet, "Determination of the orientation workspace of parallel manipulators," *J. Intell. Robot. Syst.* **13**, 143–160 (1995).
3. K. J. Waldron and A. Kumar, "The workspaces of a mechanical manipulator," *ASME J. Mech. Des.* **103**, 665–672 (1981).
4. Y. C. Tsai and A. H. Soni, "Accessible region and synthesis of robot arm," *ASME J. Mech. Des.* **103**, 803–811 (1981).
5. K. G. Gupta and B. Roth, "Design considerations for manipulator workspace," *ASME J. Mech. Des.* **104**, 704–711 (1982).
6. J. K. Davidson and K. H. Hunt, "Rigid body location and robot workspace: Some alternative manipulator forms," *ASME J. Mech. Transm.* **109**, 224–242 (1987).
7. F.-C. Yang and E. J. Haug, "Numerical analysis of the kinematic working capability of mechanisms," *ASME J. Mech. Des.* **116**, 111–118 (1994).
8. E. J. Haug, C.-M. Luh, F. A. Adkins and J.-Y. Wang, "Numerical algorithms for mapping boundaries of manipulator workspaces," *ASME J. Mech. Des.* **118**, 228–234 (1996).
9. G. T. Pond and J. A. Carretero, "Quantitative dexterous workspace comparison parallel manipulators," *Mech. Mach. Theory* **42**, 1388–1400 (2007).
10. I. A. Bonev and J. Ryu, "A new approach to orientation workspace analysis of 6-dof parallel manipulators," *Mech. Mach. Theory* **36**, 15–28 (2001).
11. K.-K. Oh, X.-J. Liu, D. S. Kang and J. Kim, "Optimal design of a micro parallel positioning platform. Part I: Kinematic analysis," *Robotica* **22**, 599–606 (2004).
12. K.-K. Oh, X.-J. Liu, D. S. Kang and J. Kim, "Optimal design of a micro parallel positioning platform. Part. II: Real machine design," *Robotica* **23**, 109–122 (2005).
13. C. Ahn, T. Seo, J. Kim and T. Kim, "High-tilt parallel positioning mechanism development and cutter path simulation for laser micro-machining," *Comput.-Aided Des.* **39**, 218–228 (2007).
14. J. Kim, F. C. Park, S. J. Ryu, J. Kim, J. Hwang, C. Park and C. Iurascu, "Design and analysis of a redundantly actuated parallel mechanism for rapid machining," *IEEE Trans. Robot. Autom.* **17**, 423–434 (2001).
15. J. Kim, K. S. Cho, J. Hwang, C. Iurascu and F. C. Park, "Eclipse-RP: A new RP machine based on deposition and machining," *J. Multi-body Dyn.* **216**, 13–20 (2002).
16. J. J. Craig, *Introduction to Robotics: Mechanics and Control*, 3rd ed. (Prentice Hall, Upper Side River, New Jersey, USA) ISBN-13: 978-0201543612.
17. S. Kucuk and Z. Bingul, "Comparative study of performance indices for fundamental robot manipulator," *Robot. Auton. Syst.* **54**, 567–573 (2006).
18. F. Hao and J.-P. Merlet, "Multi-criteria optimal design of parallel manipulators based on interval analysis," *Mech. Mach. Theory* **40**, 157–171 (2004).
19. A. Homaifar, S. H. Y. Lai and X. Qi, "Constrained optimization via genetic algorithms," *Simulation* **62**, 242–254 (1994).
20. Z. Michalewicz, "Evolutionary algorithms for constrained engineering problems," *Comput. Ind. Eng.* **30**, 851–870 (1996).

https://doi.org/10.1017/S0263574711000774 Published online by Cambridge University Press